Using Least Squares to Determine the Coefficients of the CVBEM Approximation Function

Bryce D. Wilkins[1],
Theodore V. Hromadka II[2]

[1]Carnegie Mellon University
[2]Distinguished Professor, United States Military Academy

bwilkins@andrew.cmu.edu

theodore.hromadka@westpoint.edu

October 21, 2021

Section 1

A Least Squares Approach

The General CVBEM Approximation Function

- The CVBEM approximation function is a linear combination of complex variable functions that are analytic within a given problem domain, Ω:

$$\hat{\omega}(z) = \sum_{j=1}^{n} c_j g_j(z), \quad z \in \Omega, \tag{1}$$

- where
  - $c_j = \alpha_j + i\beta_j$ are complex coefficients,
  - $g_j(z)$ are analytic complex variable basis functions,
  - n is the number of basis functions being used in the approximation

Some possible basis functions:

- $(z - z_j)\ln_{\alpha_j}(z - z_j)$
- $1/(z - z_j)$
- $(z - z_j)^j$
- Digamma
- Polygamma
- And more!

Hromadka II, T.V., Guymon, G.L., A Complex Variable Boundary Element Method: Development. *International Journal for Numerical Methods in Engineering*, pp. 25-37, 1984.

Collocation versus Least Squares

Collocation:

- In the collocation approach, each term in the approximation function corresponds to one node and two collocation points.
- Only $2n$ collocation points will be used when computing the coefficients of the CVBEM approximation function.

Least Squares:

- In the least squares approach, all of the boundary data is used when computing the coefficients of the CVBEM approximation function.

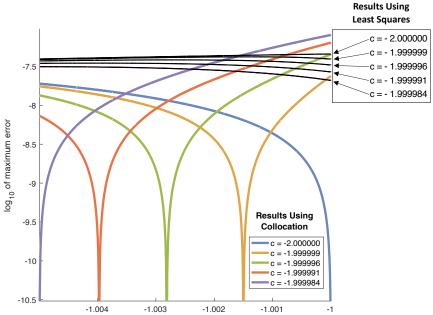

Figure: Collocation versus least squares: absolute value of approximation error for several streamlines in the vicinity of a stagnation point.

Least Squares is the Key to 3D

Collocation:

- In 3D, only selecting $2n$ collocation points when formulating the CVBEM model is not sufficient to accurately describe the governing flow situation.

Least Squares:

- We have to use least squares because it incorporates all of the available boundary data when computing the coefficients of the CVBEM approximation function.

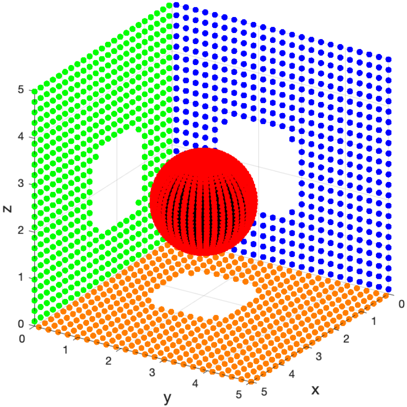

Figure: 3D problem geometry.

Node Position Algorithm (NPA)

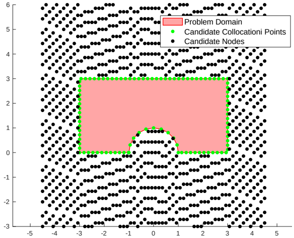

Figure: The NPA begins by establishing candidate nodes in the exterior of the problem domain. Candidate nodes are tested one-at-a-time to determine which node contributes the most to reducing the maximum error of the CVBEM approximation function.

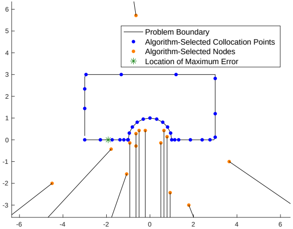

Figure: After a node is selected, the maximum error of the resulting CVBEM model is assessed on the problem boundary. Two new collocation points are added at the two highest local maxima of the error function on the boundary.

Demoes, N.J., Bann, G.T., Wilkins, B.D., Grubaugh, K.E. & Hromadka II, T.V., Optimization Algorithm for Locating Computational Nodal Points in the Method of Fundamental Solutions to Improve Computational Accuracy in Geosciences Modeling. *The Professional Geologist*, pp. 6-12, 2019.

Adapting the NPA to Composite Basis Functions

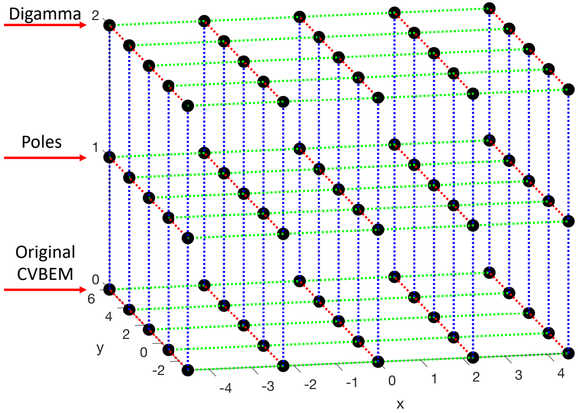

Figure: When using composite basis functions, the NPA has to determine the x and y coordinates of the node as well as the type of basis function to use. This results in a 3D search, as indicated in the figure. Each layer (in the vertical direction) of the candidate nodes corresponds to a different family of basis functions.

Mechanics of the CVBEM

The CVBEM approximation function:

$$\begin{aligned}\hat{\omega}(z) &= \sum_{j=1}^{n} c_j g_j(z)\\ &= \sum_{j=1}^{n} \left(\alpha_j + i\beta_j\right)\left(\lambda_j(x,y) + i\mu_j(x,y)\right)\\ &= \sum_{j=1}^{n} \Big[\alpha_j\lambda_j(x,y) - \beta_j\mu_j(x,y) + i\left[\alpha_j\mu_j(x,y) + \beta_j\lambda_j(x,y)\right]\Big].\end{aligned}$$

Let:

$$\boldsymbol{\alpha} = \begin{bmatrix}\alpha_1\\ \alpha_2\\ \vdots\\ \alpha_n\end{bmatrix}, \quad \boldsymbol{\beta} = \begin{bmatrix}\beta_1\\ \beta_2\\ \vdots\\ \beta_n\end{bmatrix},$$

$$\boldsymbol{\lambda} = \begin{bmatrix}\lambda_1(x,y)\\ \lambda_2(x,y)\\ \vdots\\ \lambda_n(x,y)\end{bmatrix}, \quad \boldsymbol{\mu} = \begin{bmatrix}\mu_1(x,y)\\ \mu_2(x,y)\\ \vdots\\ \mu_n(x,y)\end{bmatrix}.$$

The real and imaginary parts of the CVBEM approximation function:

$$\begin{aligned}\Re\left[\hat{\omega}(z)\right] = \hat{\phi}(x,y) &= \sum_{j=1}^{n} \alpha_j\lambda_j(x,y) - \beta_j\mu_j(x,y)\\ &= \boldsymbol{\lambda}^\top\boldsymbol{\alpha} - \boldsymbol{\mu}^\top\boldsymbol{\beta},\\ \Im\left[\hat{\omega}(z)\right] = \hat{\psi}(x,y) &= \sum_{j=1}^{n} \alpha_j\mu_j(x,y) + \beta_j\lambda_j(x,y)\\ &= \boldsymbol{\mu}^\top\boldsymbol{\alpha} + \boldsymbol{\lambda}^\top\boldsymbol{\beta}.\end{aligned}$$

In matrix form:

$$\begin{bmatrix}\hat{\phi}(x,y)\\ \hat{\psi}(x,y)\end{bmatrix} = \begin{bmatrix}\boldsymbol{\lambda}^\top & -\boldsymbol{\mu}^\top\\ \boldsymbol{\mu}^\top & \boldsymbol{\lambda}^\top\end{bmatrix}\begin{bmatrix}\boldsymbol{\alpha}\\ \boldsymbol{\beta}\end{bmatrix}.$$

Handling the Mixed Boundary Conditions

The Dirichlet boundary conditions:

$$\begin{aligned}\hat{\phi}(x_{i,\mathrm{D}}, y_{i,\mathrm{D}}) &= \sum_{j=1}^{n} \alpha_j \lambda_j(x_{i,\mathrm{D}}, y_{i,\mathrm{D}}) - \beta_j \mu_j(x_{i,\mathrm{D}}, y_{i,\mathrm{D}}) \\ &= \phi(x_{i,\mathrm{D}}, y_{i,\mathrm{D}}), \\ \text{for} \quad i &= 1, \ldots, N_{\mathrm{D}}, \quad (x_{i,\mathrm{D}}, y_{i,\mathrm{D}}) \in \partial\Omega_{\mathrm{D}}.\end{aligned}$$

The Neumann boundary conditions:

$$\begin{aligned}\hat{\psi}(x_{i,\mathrm{N}}, y_{i,\mathrm{N}}) &= \sum_{j=1}^{n} \alpha_j \mu_j(x_{i,\mathrm{N}}, y_{i,\mathrm{N}}) + \beta_j \lambda_j(x_{i,\mathrm{N}}, y_{i,\mathrm{N}}) \\ &= \text{const}, \\ \text{for} \quad i &= 1, \ldots, N_{\mathrm{N}}, \quad (x_{i,\mathrm{N}}, y_{i,\mathrm{N}}) \in \partial\Omega_{\mathrm{N}}.\end{aligned}$$

Let:

$$\mathbf{x}_{\mathrm{D}} = \begin{bmatrix} x_{1,\mathrm{D}} \\ x_{2,\mathrm{D}} \\ \vdots \\ x_{N_{\mathrm{D}},\mathrm{D}} \end{bmatrix}, \quad \mathbf{y}_{\mathrm{D}} = \begin{bmatrix} y_{1,\mathrm{D}} \\ y_{2,\mathrm{D}} \\ \vdots \\ y_{N_{\mathrm{D}},\mathrm{D}} \end{bmatrix},$$

$$\mathbf{x}_{\mathrm{N}} = \begin{bmatrix} x_{1,\mathrm{N}} \\ x_{2,\mathrm{N}} \\ \vdots \\ x_{N_{\mathrm{N}},\mathrm{N}} \end{bmatrix}, \quad \text{and} \quad \mathbf{y}_{\mathrm{N}} = \begin{bmatrix} y_{1,\mathrm{N}} \\ y_{2,\mathrm{N}} \\ \vdots \\ y_{N_{\mathrm{N}},\mathrm{N}} \end{bmatrix}.$$

In matrix form:

$$\begin{bmatrix} \underbrace{\phi\left(\mathbf{x}_{\mathrm{D}}, \mathbf{y}_{\mathrm{D}}\right)}_{N_{\mathrm{D}} \times 1} \\ \underbrace{\mathbf{f}}_{N_{\mathrm{N}} \times 1} \end{bmatrix} = \begin{bmatrix} \underbrace{\lambda\left(\mathbf{x}_{\mathrm{D}}, \mathbf{y}_{\mathrm{D}}\right)}_{N_{\mathrm{D}} \times n} & \underbrace{-\mu\left(\mathbf{x}_{\mathrm{D}}, \mathbf{y}_{\mathrm{D}}\right)}_{N_{\mathrm{D}} \times n} \\ \underbrace{\mu\left(\mathbf{x}_{\mathrm{N}}, \mathbf{y}_{\mathrm{N}}\right)}_{N_{\mathrm{N}} \times n} & \underbrace{\lambda\left(\mathbf{x}_{\mathrm{N}}, \mathbf{y}_{\mathrm{N}}\right)}_{N_{\mathrm{N}} \times n} \end{bmatrix} \begin{bmatrix} \underbrace{\boldsymbol{\alpha}}_{n \times 1} \\ \underbrace{\boldsymbol{\beta}}_{n \times 1} \end{bmatrix},$$

$$\text{where } \mathbf{f} = \gamma \begin{bmatrix} 1 \\ 1 \\ 1 \\ \vdots \\ 1 \end{bmatrix}, \quad \gamma \in \mathbb{R}.$$

Section 2

Example Problem and Results

Example Problem Details

Problem Domain:	$\Omega = \left\{ (x,y):\ 0 < x < 13,\ 0 < y < 6, \text{ and } (x-3)^2 + y^2 > 1 \text{ and } (x-8)^2 + y^2 > 1 \right\}$
Governing PDE:	$\nabla^2 \phi = 0$
Boundary Conditions:	$\begin{cases} \frac{\partial \phi}{\partial n} = 0, & x = 0 \\ \frac{\partial \phi}{\partial n} = 0, & y = 0 \\ \frac{\partial \phi}{\partial n} = 0, & (x-3)^2 + y^2 = 1 \\ \frac{\partial \phi}{\partial n} = 0, & (x-8)^2 + y^2 = 1 \\ \phi(x,y) = \Re\left[z^2\right] = x^2 - y^2, & \text{otherwise} \end{cases}$
Number of Candidate Computational Nodes:	2,000
Number of Candidate Collocation Points:	2,000

CVBEM Modeling Outcomes

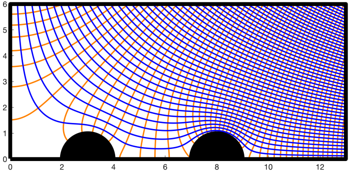

Figure: CVBEM-produced flownet depicting the entire problem domain. The CVBEM model was developed using composite-type basis functions.

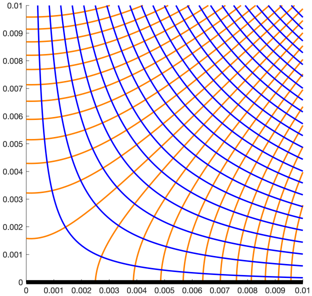

Figure: CVBEM-produced flownet near the origin where we observe potential flow in a 90-degree bend. Here, the flow situation is computationally difficult to model because of the relatively extreme curvature of the flow regime.

CVBEM Modeling Outcomes (continued)

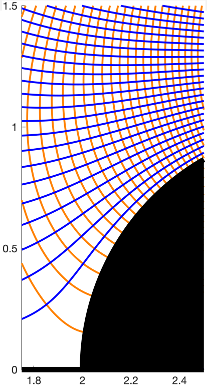

Figure: CVBEM-produced flownet near the left edge of the left cylindrical obstacle.

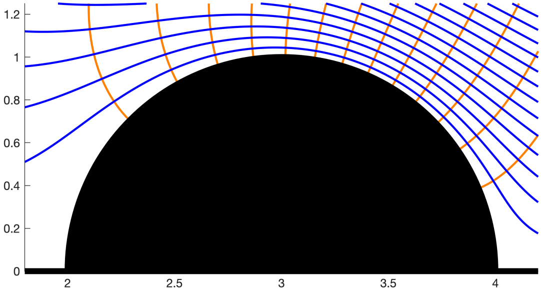

Figure: CVBEM-produced flownet near the left obstacle. The north pole of the obstacle, as well as the left and right edges of the obstacle, are areas of interest due to the relatively extreme nature of the curvature of the flow situation in those areas.

CVBEM Modeling Outcomes (continued)

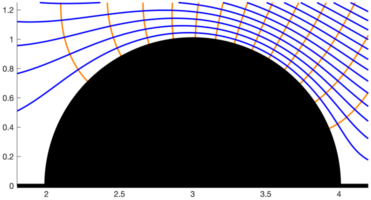

Figure: CVBEM-produced flownet near the left cylinder.

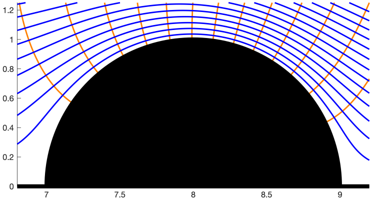

Figure: CVBEM-produced flownet near the right cylinder.

Error Results

Figure: Maximum absolute error of CVBEM models created using composite basis functions (standard CVBEM, digamma, poles). The maximum error is reported as each new node is added to the CVBEM model up to a total of 120 nodes. Approximately 120 nodes are needed to reach our target maximum error of 10^{-6}. These results were obtained using a least squares implementation of the CVBEM.

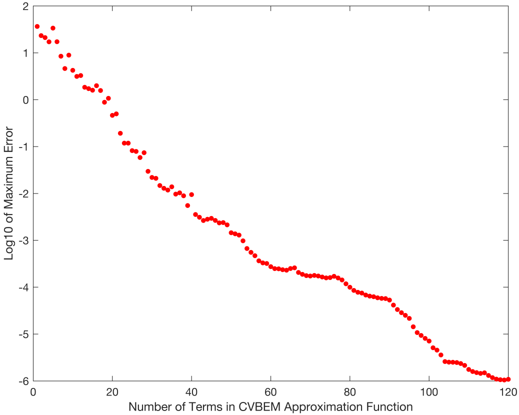

Section 3

Final Thoughts - Line Search Technique

Line-search approach

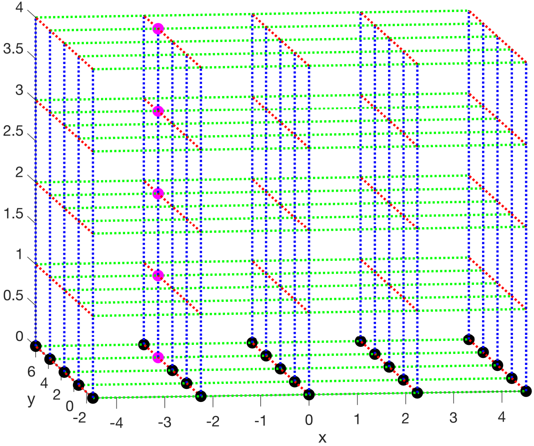

Figure: An alternative to the 3D search method is to apply the standard 2D search method while only considering one family of basis functions. Once the "best" location has been determined, then that location can be held fixed as the NPA tests each candidate basis function family at that location to see which family results in the CVBEM model of least error.

Questions

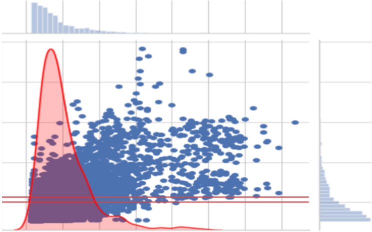

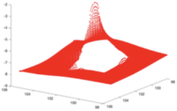

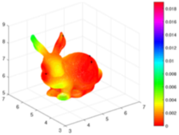

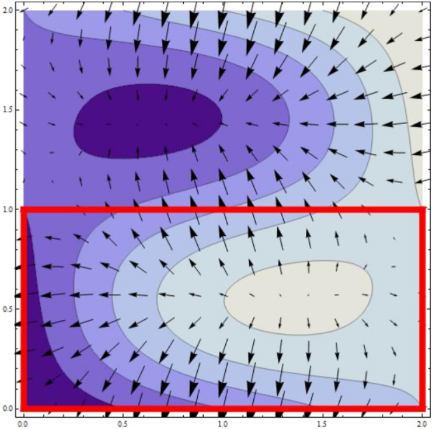
2.0
1.5
1.0
0.5
0.0
0.0
0.5
1.0
1.5
2.0